A Waveguide Power Transfer for Electric Vehicles in Motion

Yuichi Masuda [1,2] Naoya Takahashi [3] Katsuhiro Hata [3] Hiroyuki Shinoda [1]

1) The University of Tokyo, Graduate school of Frontier Sciences, 5-1-5 Kashiwanoha, Kashiwa-shi, Chiba, Japan

E-mail: masuda@hapis.k.u-tokyo.ac.jp, hiroyuki_shinoda@k.u-tokyo.ac.jp

2) 2DC, Inc., 1-12-4 Ginza, Chuo-ku, Tokyo, Japan

E-mail: masuda@2dc.co.jp

3) Shibaura Institute of Technology, College of Engineering, 3-7-5 Toyosu, Koto-ku, Tokyo, 135-8548, Japan

E-mail: ag22054@shibaura-it.ac.jp, khata@shibaura-it.ac.jp

ABSTRACT: We propose a waveguide power transfer system for electric vehicles (EVs) in motion. In conventional wireless power transfer systems using magnetic coupling, the coupling coefficient tends to decrease due to flux leakage, which limits the positional flexibility of the receiver. The proposed system addresses this limitation by significantly reducing the group velocity in a waveguide sheet, allowing for strong magnetic coupling to be maintained regardless of the waveguide sheet length. We introduce a theoretical framework that considers three critical areas: propagation, coupling, and termination. Experimental results at 85 kHz confirmed wave propagation characteristics, achieving maximum power transfer efficiencies of approximately 86 %.

KEY WORDS: wireless power transfer, waveguide power transfer, magnetic coupling, electromagnetic compatibility (EMC)

1. INTRODUCTION

The trade-off between coil alignment and coupling efficiency presents a significant challenge in wireless power transfer (WPT) systems that utilize magnetic coupling. [1] [2] In applications such as dynamic wireless power transfer for electric vehicles (EVs), where both extended power transfer range and high efficiency are essential, this challenge is addressed by strategically driving multiple power transfer coils. [3] - [6]

An alternative solution is waveguide-based power transfer. [7][8] In this approach, electromagnetic waves are propagated within a waveguide sheet, and power is extracted by receiving coils located nearby. By utilizing propagation and coupling mechanisms, both extensive range and high efficiency can be achieved.

In this paper, we propose a magnetically coupled waveguide power transfer [9]. Fig. 1 shows a conceptual diagram of this scheme. The propagation within the waveguide sheet is characterized by significantly slowed group velocity. Electromagnetic energy propagates gradually along the sheet.

Thus, the waveguide sheet is divided into three regions: propagating, coupled, and terminating. The extent of the coupling region is dictated by the group velocity, ensuring constant coupling strength regardless of waveguide length. Note that "waveguide power transfer" in this paper refers specifically to WPT via electromagnetic waves propagating along a sheet-like medium, as shown in Fig. 1.

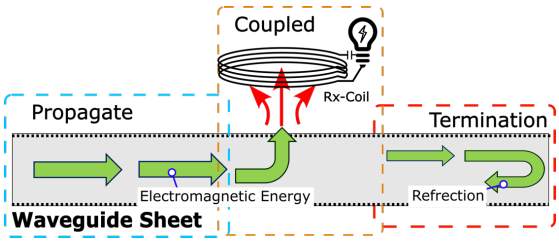

Fig. 1 Schematic of the waveguide method. Extending the waveguide mainly affects the propagation area, not the coupling region. Part of the electromagnetic wave reaches the waveguide end and is reflected.

This paper is organized as follows. Section 2 introduces an equivalent lumped-element circuit model of the proposed scheme and analyzes it based on magnetic resonance theory. [10] Section 3 presents a prototype waveguide sheet and its characteristics measurement results. Section 4 concludes this paper.

2. WAVEGUIDE POWER TRANSFER

2.1. Equivalent Circuit

Fig. 2 presents an equivalent circuit model of the waveguide method. In this model, the waveguide within the propagation region is represented by a transmission line with a characteristic impedance denoted as R_s. The coupling region is modeled as a magnetically coupled circuit, consisting of both the waveguide coil structure and the receiving coil. The mutual inductance L_m is calculated using the respective inductances L_{TX} and L_{RX}, along with the coupling coefficient k, and is expressed by the following:

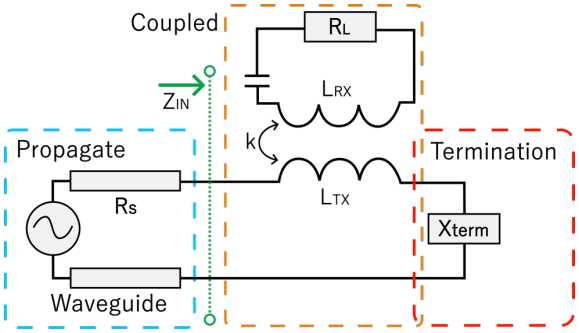

Fig. 2 Equivalent circuit of the waveguide method. The termination area is represented by a reactance element. Due to its similarity to the S-S magnetic resonance circuit, there is a high potential for applying established theoretical frameworks.

$$L_m = k\sqrt{L_{TX}L_{RX}}\,. \tag{1}$$

2.2. Coupling and Termination

In the equivalent circuit model, the termination region is substituted with a reactance element X_{term}. When resonance conditions (2) and (3) are met, the coupling and terminating regions together function as an S-S resonant circuit. [10]

$$\omega L_{TX} + X_{term} = 0\,, \tag{2}$$

$$\omega L_{RX} - \frac{1}{\omega C_{RX}} = 0\,. \tag{3}$$

Note that ω represents the angular frequency, and C_{RX} is the capacitance required for series resonance in the receiving coil. The coupling efficiency η_c and the coupling region's input impedance Z_{IN} are given by the following equations:

$$\eta_c = \frac{R_L(\omega L_m)^2}{r_{TX}(R_L + r_{RX})^2 + r_{RX}(\omega L_m)^2 + R_L(\omega L_m)^2}\,, \tag{4}$$

$$Z_{IN} = \frac{(\omega L_m)^2}{R_L + r_{RX}} + r_{TX}\,. \tag{5}$$

In the model, r_{TX}, r_{RX} and R_L represent the resistances of the waveguide sheet, receiving coil and load within the coupling region, respectively. Similar to the S-S scheme, both the coupling coefficient and the quality factor significantly influence the efficiency of the power supply. Note that reflections occur within the waveguide if Z_{IN} deviates from the characteristic impedance R_s.

2.3. Propagate

The group velocity v_g in the propagation region is given by (6), and the attenuation coefficient α is defined in (7).

$$v_g = \frac{\partial\omega(k_1)}{\partial k_1}\,, \tag{6}$$

$$\alpha = \frac{k_1 R_o}{2\omega L_o}. \tag{7}$$

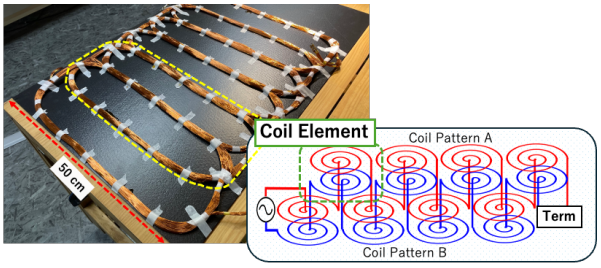

Fig. 3 Prototype waveguide. Coil elements are serially interconnected. The waveguide length can be extended by longitudinally connecting an additional waveguide.

The wavenumber k_1 characterizes the electromagnetic wave propagating in the waveguide, while R_o and L_o represent the resistance and inductance of the waveguide per unit distance, respectively.

According to (6) and (7), the wavenumber k_1 determines the group velocity and propagation loss. A larger k_1 slows down the group velocity, effectively narrowing the coupling region and improving efficiency due to reduced flux leakage. However, this slower propagation also results in higher propagation losses, highlighting an inherent trade-off. Thus, the optimal choice of k_1 balances coupling efficiency and propagation loss.

3. EXPERIMENTAL RESULT

In this section, we evaluate the feasibility of waveguide power transfer at 85 kHz. A prototype scaled for implementation in vehicles and road infrastructures was developed and evaluated in terms of propagation efficiency, load characteristics, positional flexibility, and air-gap tolerance.

3.1. Propagation Efficiency

Fig. 3 illustrates the prototype waveguide sheet along with its simplified structural model. The waveguide sheet operates as a transmission line, composed of continuously distributed inductors and capacitors, realized by connecting multiple coil elements in series. Each coil element comprises two coils wound in opposite directions and driven by currents of differing phases, creating a uniform magnetic field. To enhance field uniformity, the coil patterns partially overlap, forming capacitances between patterns A and B.

Table 1 summarizes the waveguide's characteristics and propagation efficiency η_p, determined by measuring input and output power using a power analyzer (HIOKI, PW8001) with the waveguide terminated by a matched, non-inductive load. A sinusoidal signal provided by a high-speed bipolar amplifier (NF Corporation, HSA42014) was used during the measurements. The propagation efficiency measured at various frequencies is shown in Fig. 4.

Table 1 Properties of Prototyped Waveguide.

Var.	Description	Value
f	Electromagnetic wave frequency [kHz]	85
l	Length of waveguide sheet [m]	1.3
R_o	Resistance per unit distance [Ω/m]	1.02
L_o	Inductance per unit distance [μH/m]	125
C_o	Capacitance per unit distance [nF/m]	278
Q	Q value at 85 kHz	69.8
R_s	Characteristic impedance [Ω]	21.3
λ	Wavelength [m]	2
k_1	Wave number	3.148
v_g	Group velocity [m/s]	170,000
η_p	Propagation efficiency [%/m]	89.2

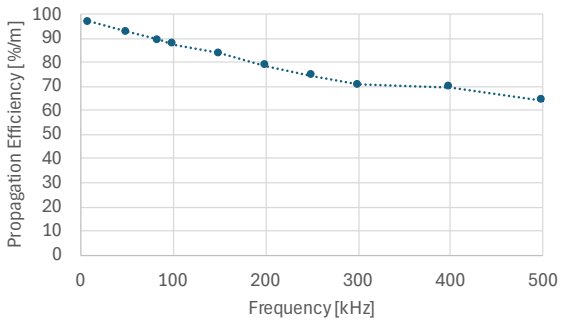

Fig. 4 Propagation efficiency per unit length at various frequencies. Efficiency decreases at higher frequencies due to shorter wavelengths within the waveguide sheet.

Within the waveguide, the wavelength λ and group velocity v_g are significantly reduced—approximately 1/1750 of their free-space values. As a result, electromagnetic energy propagates slowly along the sheet, advancing about 2 m per cycle. This slow propagation ensures a stable coupling strength between the waveguide sheet and receiving coil, unaffected by the length of the waveguide.

Table 2 Properties of Receiving Coil.

Var.	Description	Value
f	Resonance frequency [kHz]	85
R_{RX}	Resistance [Ω]	1.2
L_{RX}	Inductance [μH]	603
Q	Q value at 85 kHz	257
	Optimum load impedance [Ω]	12
	Airgap [mm]	100
	Outer diameter [mm]	450
	Turns	48
	Specifications of wire	KIV 2.0 sq

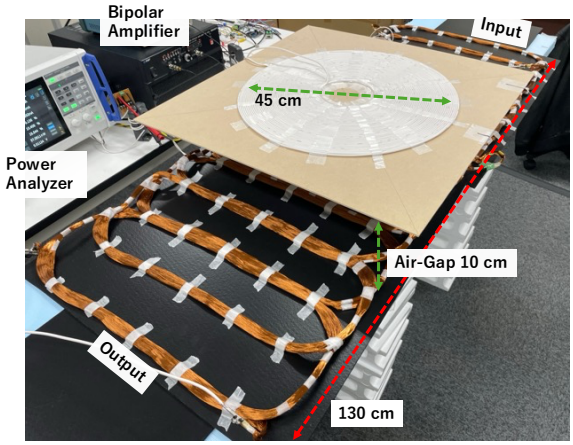

Fig. 5 Experimental setup for evaluating load characteristics. The receiving coil is positioned at a standing-wave peak, and the waveguide sheet is shorted-terminated.

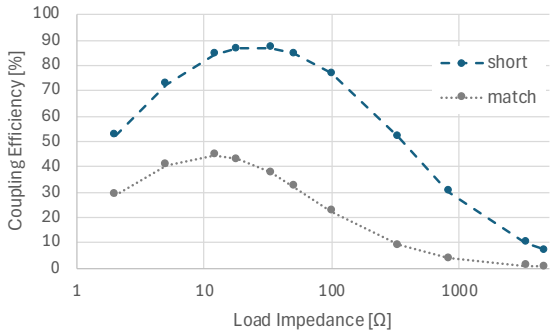

Fig. 6 Power transfer efficiency versus load resistance.

At lower frequencies, longer wavelengths within the waveguide sheet improve propagation efficiency η_p. However, this simultaneously expands the coupling region, reducing the coupling efficiency η_c. Thus, an optimal system design must balance both efficiencies.

3.2. Load Characteristics

Similar to magnetic resonance, coupling efficiency η_c can be optimized by appropriately designing the load impedance R_L. Coupling efficiency was measured under varying R_L for two termination conditions: shorted and matched. In the shorted-terminated case, the receiving coil was positioned at a standing-wave peak (x = 20 cm in Fig. 7), while for the matched-terminated case, the coil was placed at the center of the waveguide sheet. The air-gap distance was fixed at 100 mm in both measurements.

The experimental setup is shown in Fig. 5, and measurement results are presented in Fig. 6. For the shorted termination, the receiving coil position satisfies the resonance condition given by (2), maximizing η_c. Under this condition, η_c reaches its maximum of 86.9 % at a load resistance of 33 Ω. At a significantly higher load (4700 Ω), η_c drops to approximately 7.25 %, and according to (5),

the input impedance Z_{IN} is dominated by r_{TX}. Consequently, the coupled-termination region behaves effectively as a shorted termination.

For the matched termination, η_c reaches its maximum at a load resistance of 12 Ω. At a significantly higher load resistance (4700 Ω), η_c decreases to below 1%. Under this condition, most electromagnetic energy is not extracted by the receiving coil and is instead absorbed by the matched termination.

Note that for the matched termination, the theoretical η_c is limited to 50 % due to the symmetric configuration around the receiving coil [9]. Shorted or open-ended terminations break this symmetry condition, enabling a theoretical maximum η_c of 100 %.

3.3. Positional Flexibility

Power transfer efficiency, defined here as the ratio of the output power at the receiving coil load to the input power supplied to the waveguide sheet, was measured at different positions along the waveguide.

Measurements were conducted under three termination conditions: matched, shorted, and open-ended, with the optimal load resistance for each termination condition. The experimental setup is shown in Fig. 7. The receiving coil was moved in 10-cm increments along the waveguide, maintaining an air gap of 100 mm. Measurement results are presented in Fig. 8.

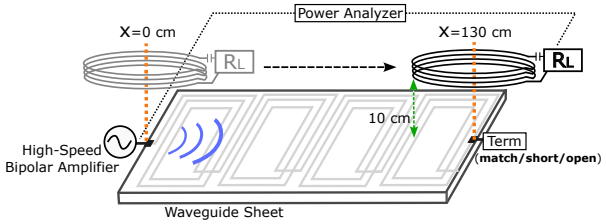

Fig. 7 Experimental setup. Measurements are conducted at 10 cm intervals along the waveguide, using the coil center as a reference point, under matched, shorted, and open-ended termination conditions.

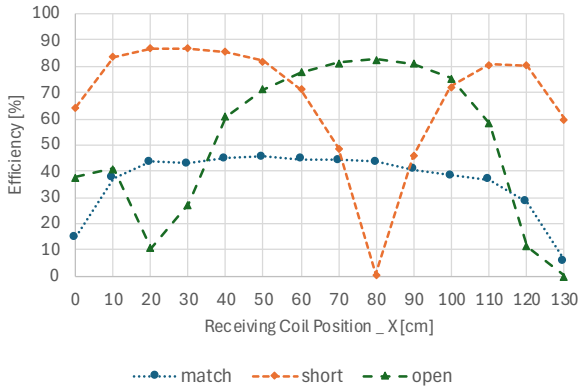

Fig. 8 Power transfer efficiency at various receiving coil positions. Measurements were conducted under matched, shorted, and open-ended terminations, with efficiency calculated from input and receiving coil output power.

With shorted and open-ended terminations, standing waves form within the waveguide sheet, resulting in alternating regions of high and low efficiency. High-efficiency peaks occur at positions satisfying the resonance condition described by equation (2). Switching between shorted and open-ended terminations reverses the positions of these peaks and troughs. By suitably selecting the termination type, power transfer efficiency ranging from approximately 80 to 86 % can be achieved across nearly the entire waveguide area.

In contrast, the matched termination prevents reflections, eliminating standing waves and producing a relatively uniform efficiency distribution. Efficiency gradually decreases with increasing distance from the input port due to propagation losses. Note that efficiency declines near the sheet edges as the receiving coil partially extends beyond the waveguide sheet area.

3.4. Air Gap

To evaluate the effect of the air gap between the waveguide and receiving coil on power transfer efficiency, measurements were conducted at the highest efficiency position (shorted termination, x = 20 cm in Fig. 8), varying the air gap from 50 mm to 250 mm in 50 mm increments. Load resistance and other experimental conditions remained consistent with previous experiments. The results (Fig. 7) show that efficiency gradually decreases for gaps exceeding 150 mm, with approximately a 10 % drop at 200 mm compared to the efficiency at a 100 mm gap.

The mutual inductance between the waveguide and the receiving coil varies with the air-gap distance. Thus, selecting the optimal load impedance according to each air-gap distance could potentially maintain higher power transfer efficiency.

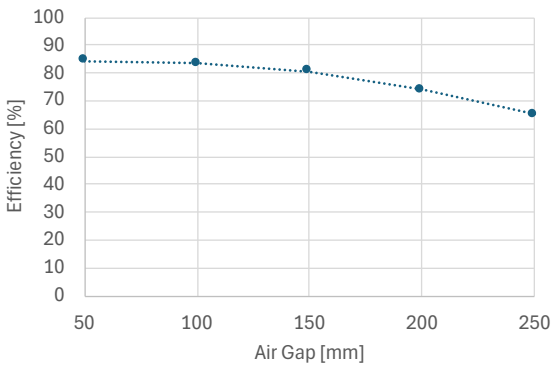

Fig. 9 Power transfer efficiency versus air gap, measured at x = 20 cm with shorted termination.

4. CONCLUSIONS

In this paper, we proposed a magnetically coupled waveguide power transfer system for dynamic wireless power transfer applications, addressing the positional flexibility limitations and efficiency losses typically associated with flux leakage. By significantly reducing the group velocity of electromagnetic waves propagating along a waveguide sheet, the proposed system separates the propagation, coupling, and termination regions. As the coupling strength remains independent of waveguide length, positional flexibility can be extended without compromising efficiency.

We experimentally demonstrated the feasibility of this approach through a prototype operating at 85 kHz. Experiments evaluated propagation efficiency, load characteristics, positional flexibility, and air-gap dependence. Consistent with magnetic resonance methods, optimizing the receiving coil load significantly improved power transfer efficiency. Efficiency was also found to vary distinctly with different termination conditions.

Matched termination resulted in relatively uniform efficiency, whereas shorted and open-ended terminations produced clear standing-wave patterns. By appropriately switching between shorted and open-ended terminations, efficiencies of approximately 80–86 % were achievable across most of the waveguide sheet. Additionally, increasing the air gap up to 200 mm reduced efficiency by no more than 10 %.

Future work will focus on enhancing the quality factor of the waveguide sheet by refining coil pattern structures, aiming to further improve both propagation efficiency and coupling efficiency.

ACKNOWLEDGMENT

THIS WORK WAS SUPPORTED BY JSPS KAKENHI GRANT NUMBER 21K14155.

REFERENCES

(1) R. Bosshard, U. Iruretagoyena and J. W. Kolar, “Comprehensive evaluation of rectangular and double-D coil geometry for 50 kW/85 kHz IPT system,” in IEEE Journal of Emerging and Selected Topics in Power Electronics, vol. 4, no. 4, pp. 1406-1415, Dec. 2016.

(2) Y. Li, J. Zhao, Q. Yang, L. Liu, J. Ma and X. Zhang, “A novel coil with high misalignment tolerance for wireless power transfer,” in IEEE Transactions on Magnetics, vol. 55, no. 6, pp. 1-4, June 2019.

(3) A. Mahesh, B. Chokkalingam and L. Mihet-Popa, “Inductive wireless power transfer charging for electric vehicles–a review,” in IEEE Access, vol. 9, pp. 137667-137713, 2021.

(4) T. Fujita, T. Yasuda and H. Akagi, “A dynamic wireless power transfer system applicable to a stationary system,” in IEEE Transactions on Industry Applications, vol. 53, no. 4, pp. 3748-3757, July-Aug. 2017.

(5) S. Laporte, G. Coquery, V. Deniau, A. De Bernardinis, and N. Hautiere, “Dynamic wireless power transfer charging infrastructure for future EVs: From experimental track to real circulated roads demonstrations,” World Electric Vehicle Journal, vol. 10, no. 4, pp. 84, 2019.

(6) J. Rahulkumar. et al., “An empirical survey on wireless inductive power pad and resonant magnetic field coupling for in-motion EV charging system,” IEEE Access, vol. 11, pp. 4660-4693, 2023.

(7) H. Shinoda, Y. Makino, N. Yamahira and H. Itai, “Surface sensor network using inductive signal transmission layer,” 2007 Fourth International Conference on Networked Sensing Systems, Braunschweig, Germany, 2007, pp. 201-206.

(8) A. Noda and H. Shinoda, “Selective wireless power transmission through high- Q flat waveguide-ring resonator on 2-D waveguide sheet,” in IEEE Transactions on Microwave Theory and Techniques, vol. 59, no. 8, pp. 2158-2167, Aug. 2011.

(9) Y. Masuda and H. Shinoda, “A magnetically coupled 2-D waveguide power transfer,” IECON 2024-50th Annual Conference of the IEEE Industrial Electronics Society. IEEE, 2024.

(10) T. Imura and Y. Hori, " Unified theory of electromagnetic induction and magnetic resonant coupling," in IEEJ Transactions on industry applications, vol. 199, no. 2, pp. 58-80, April 2017.